LOW TEMPERATURE CARBOTHERMAL REDUCTION OF SILICEOUS MANGANESE FINES

R. Kononov[1], O. Ostrovski[1] and S. Ganguly[2]

[1] School of Materials Science and Engineering, the University of New South Wales, Sydney, NSW 2052, Australia; o.ostrovski@unsw.edu.au
[2] Hatch, 61 Petrie Terrace, Brisbane, Australia; sganguly@hatch.com.au

ABSTRACT

The paper examines carbothermal reduction of Groote Eylandt siliceous manganese fines with 34.4 wt% SiO_2 in temperature programmed and isothermal experiments in inert gas atmospheres and hydrogen.
In the temperature-programmed experiments, the first reduction stage in an inert atmosphere was conversion of MnO_2 and Mn_2O_3 to Mn_3O_4 and higher iron oxides to "FeO"; it started at about 400°C. In the second reduction stage, Mn_3O_4 was reduced to MnO and iron oxides to metallic iron. These two stages were indistinguishable and combined into one in reduction in hydrogen, which began at 300°C.

The conversion of manganese oxides to MnO and iron oxides to metallic iron at temperatures above 1000°C overlapped with reduction of MnO to ferro-manganese carbide. This process slowed down at about 1180°C, when molten slag started to form. The rate of MnO reduction from molten slag peaked at 1400°C. Silica was also reduced from the molten slag at high temperatures.

In reduction experiments in hydrogen, higher manganese oxides were reduced to MnO and iron oxides to Fe by hydrogen at temperatures below 900°C with the formation of water vapour while at higher temperatures, reduction predominantly proceeded by carbon. The rate of this stage in hydrogen was faster than in inert gas and completed at around 1150°C before the molten phase started to form.

Isothermal experiments were conducted at 1100-1200°C. The rate and degree of reduction of manganese ore increased with increasing temperature from 1100°C to 1200°C. Reduction was faster in helium than in argon, and much faster in hydrogen than in helium. In the process of carbothermal reduction of ore in hydrogen at 1200°C, silica was reduced. Reduction of the ore in hydrogen was faster than of pure MnO, particularly at 1100°C.

1 INTRODUCTION

The manganese ore body on Groote Eylandt is typically mined as two different layers - a layer of high-grade ore, and a bottom layer of high silica ore. The high silica ore (siliceous manganese fines) contains 30-35 wt% SiO_2, what is much higher than in a typical manganese ore. Chemical composition of the ore which was examined in this paper is presented in Table 1. This ore can be an appropriate source of manganese and silicon in production of silicomanganese alloy. Charge materials in silicomanganese production often include ferromanganese slag which is formed in the production of high carbon ferromanganese (HCFeMn). This slag contains 35-45 wt% MnO and 15-30 wt% SiO_2[1]. Groote Eyland siliceous fines (GE-PS) have a higher concentration of both, manganese and silicon oxides.

Smelting/reduction processes require high temperatures, about 1500°C in production of HC FeMn and above 1600°C in production of silicomanganese (SiMn). High temperatures for production of manganese alloys is first of all dictated by the temperature needed for carbothermal reduction of MnO and SiO_2. At high temperatures of industrial production of manganese alloys, manganese ore consists of two phases, one of them is solid MnO or MnO-MgO solid solution and another is molten slag[1]. Actually, reduction includes processes of MnO dissolution into the molten slag and reduction of MnO from the molten slag[2-6]. Solubility of MnO in the molten slag is near 40 wt% (depending on temperature and slag composition). When a separate MnO phase disappears in the course of

reduction, thermodynamic activity of MnO decreases approaching the equilibrium value[6,7]. This practically stops the reduction reaction although the MnO concentration in the slag is high, close to the saturation value.

A study of carbothermal reduction of manganese ores[8, 9] showed that increasing silica content in the ore adversely affects the kinetics of reduction of manganese oxide; it decreases the slag melting temperature, increases MnO concentration in the saturated with MnO slag and decreases the MnO activity coefficient.

If the reduction can occur at low temperatures, when the prevailing phase in the ore is MnO oxide or MnO-MgO solid solution, the MnO phase in the ore will be reduced directly without being dissolved in the molten slag. It was shown [10] that MnO reduction in the hydrogen atmosphere is feasible at 1200°C.

This paper studied phase composition of GE-PS ore, its change with temperature, and reduction of the ore in hydrogen. The aim of the paper is to establish reduction properties of GE-PS ore at relatively low temperatures in the range 1100-1200°C.

2 EXPERIMENTAL

Ore chemical composition was determined by the XRF method; it is given in Table 1. The ore size fraction was 45 -150μm.

Table 1 Chemical composition of manganese ore

Chemical composition, wt%							
MnO	FeO	SiO_2	Al_2O_3	CaO	MgO	BaO	K_2O
50.2	5.93	34.4	3.27	0.11	<0.1	0.75	0.51

Samples of manganese ore were analysed by XRD, optical and electron microscopy**.** X-ray diffraction was done using a Siemens D5000 X-Ray diffractometer with a Cu-Kα X-ray source and a nickel monochromator. The scans were done from 20° to 70° at 1°/min and a step size of 0.02°. The voltage used was 30 kV, with a current of 30 mA. The XRD patterns were analysed qualitatively using "Traces" software from Diffraction Technology Pty. Ltd., with JCPDS-PDF2 database.

Samples for optical and electron microscope analyses were prepared by mounting in an epoxy resin mould. These moulds were prepared by drilling through an epoxy blank, and filling the holes with the ore. Resin was then poured over the top of the blank and sample, and mixed with the sample to ensure that the particles were tightly held. The samples were held within a vacuum chamber for around 30 minutes before being left to harden for around 24 hours.

The samples were then ground using SiC paper, from 120 to 4000 grade; followed 4 μm, 1 μm and 0.5 μm diamond paste on a polishing wheel. The samples were washed using soap and water in an ultrasonic bath between the grinding and polishing, before being rinsed under ethanol. Optical photomicrographs were obtained using a Nikon Epiphot 200 (Nikon Corp., Japan) inverted stage metallurgical microscope with an attached Nikon DXM1200 digital camera. Images were captured using the Nikon ACT-1 software package.

Samples were coated with carbon for SEM, EDS and EPMA analysis. Scanning electron microscopy (SEM) was carried out using a high resolution (1.5 nm) Hitachi S-4500 field emission SEM (FESEM) with a tilting stage, Robinson back-scatter detector and Oxford Instruments cathodoluminescence detector (MonoCL2/ ISIS). FESEM was used to observe the morphologies and section profile of samples obtained at different reaction stages. Energy dispersive X-ray spectroscopy (EDS) was done using an Oxford Instruments Isis energy dispersive x-ray analyser. This was used to perform qualitative and semi-quantitative chemical analysis at different points and areas within the samples.

The mounted samples were analysed using the Cameca SX-50 electron microprobe. Standard operating procedure involved a 15 kV accelerating voltage, 1-3μm beam size and a 20nA beam current. The microprobe has four multi-crystal wavelength-dispersive spectrometers and was operated with a configuration involving two TAP, and LIF and one PET diffracting crystals.

Samples for reduction experiments were prepared by mixing synthetic graphite powder < 20 microns with manganese ores in different proportions. The gases used in these experiments were high purity argon, ultra high purity hydrogen, high purity helium, and carbon monoxide which were all supplied by Linde (Fairfield, Australia). The gases were passed through traps filled with Drierite and a 4A molecular sieve for purification and removal of moisture.

Composition of the gas introduced into the reactor was controlled by mass flow controllers. Four mass flow controllers (5850E Brooks Instruments) regulated the gas flow rates of argon, hydrogen, helium and carbon monoxide.

Experiments were conducted in a vertical tube furnace with Kanthal Super 1800-$MoSi_2$ resistance-heating elements. A schematic of the experimental set up is presented elsewhere[10]. The off-gas in isothermal experiments was analysed on-line using a CO-CO_2 infrared analyser "Advance Optima" (Hartmann & Braun, Austria). The instrument was calibrated using standard gas mixtures. The analyser was connected to the reactor off-gas outlet through the series of filters to reduce contamination of the infrared sensors.

The H_2O content was measured using a dew point monitor General Eastern Hygro M4/D-2, manufactured by General Eastern (Woburn, USA). The detecting range of the dew point monitor was –35°C to +25°C at ambient temperature of 25°C with an accuracy of 0.2°C.

A 1 gram mixture of manganese ore with graphite of known proportion was placed in a graphite crucible. Then the total weight was measured and a sample was introduced to the reactor, which was sealed and flushed with working gas at room temperature for 10 minutes before it was moved down to the hot zone from the top of the furnace. The time was noted when the reactor was placed into the hot zone of the furnace. The temperature inside the reactor was monitored by a type-B thermocouple placed just above the crucible. The total flow rate of the gas was kept at 1.2 L/min in all experiments.

After reaction, the reactor was removed from the furnace to quench the sample. When the reactor had cooled to room temperature, the crucible was extracted and the total weight was taken again to measure the weight loss of the sample. The reduced sample was taken from the crucible and prepared for further analysis by XRD, Optical microscopy, SEM, EPMA and LECO analyses as described above.

Equilibrium phases in the ore in the temperature range 800-1200°C in air and hydrogen atmosphere and in the ore-graphite mixture in hydrogen at 1100-1200°C were analysed using thermochemical software FactSage (version 6.0 with a database developed by Tang and Olsen [11]).

3 RESULTS

3.1 Phase Composition

The feature of Groote Eylandt GE-PS ore is high silica concentration, 34.4 wt%. The main phases detected by XRD were MnO_2 (pyrolusite) and quartz SiO_2. Macroscopic and microscopic investigation revealed the complex mineralogical structure of the GE-PS ore. Grains in the GE-PS ore can be divided into three main groups: manganese oxides, iron silicates and silica. Manganese oxide appeared in two modifications which were distinguished by colour; light blue particles (pyrolusite) and dark-green particles with a banded structure, identified as cryptomeline (Table 2). Manganese oxide was also a major phase in dark-blue particles, which contained alumina, silica, iron and potassium oxide and other impurities.

These impurities were also observed in other manganese oxide particles. Iron in the GE-PS ore was found mostly in the form of iron-aluminium silicate with the chemical composition matching almandine.

Upon heating in air at 1000°C high manganese oxide MnO_2 decomposed to Mn_2O_3 and Mn_3O_4 while heating in argon reduced MnO_2 to Mn_3O_4. In hydrogen, higher manganese oxides were reduced to MnO and iron oxides to metallic iron. This is seen in Figure 1 which presents the XRD patterns of ore sintered in air, argon and hydrogen. These reduction reactions during heating to 1000°C were very fast and completed in the first 10 min of the experiment.

Table 2 Selected grains of GE-PS ore and their typical composition, at%.

Colour	Phase	Mn	Fe	Si	Al	K	O
Light blue	MnO_2 oxide	27.8 28.0 28.0	0.27 0.24 0.19	0.37 0.51 0.46	0.30 0.44 0.27	0.02 0.06 0.01	66.1 66.6 66.7
Banded structure	MnO_2 oxide	30.5 30.0 29.8	0.39 0.35 0.25	0.41 0.20 0.40	0.37 0.63 0.42	0.16 0.32 0.19	65.7 65.9 63.9
Dark blue	Cryptomelane $K_xMn^{4+}_{8-x}Mn^{2+}_xO_{16}$	29.9 32.5 31.2	0.47 1.01 0.99	0.38 0.35 0.32	0.84 1.01 1.01	2.57 0.96 1.03	63.0 59.7 59.8
Red, Orange	Iron alumo-silicate	0.02 - -	18.7 16.6 17.2	8.02 8.45 8.31	8.02 8.54 8.41	1.32 1.89 1.62	63.3 63.9 63.7
Trans-parent	SiO_2	0.03 0.02 0.01	0.02 - 0.01	31.2 29.7 31.3	0.01 0.01 -	- - -	68.7 70.3 68.6

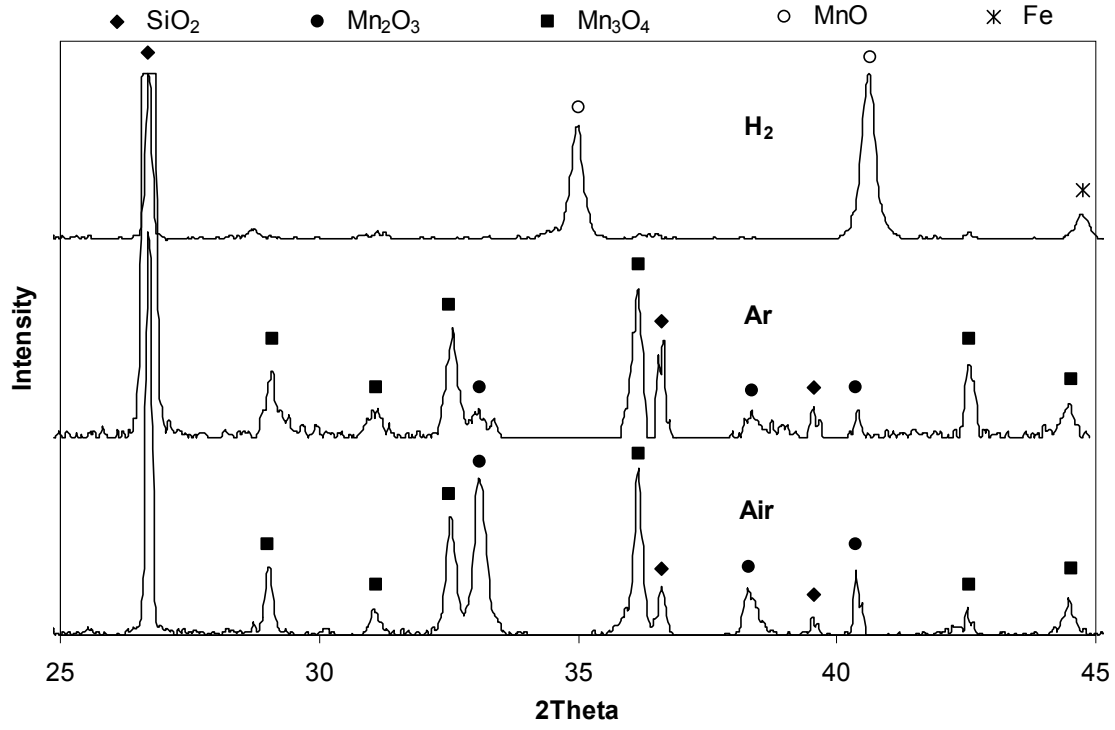

Figure 1: XRD patterns of the GE-PS ore sintered in air, argon and hydrogen at 1000°C for 60 min.

Behaviour of the sintered ore was further tested at 1200°C in hydrogen and helium. XRD spectra of the GE-PS ore sintered in helium and hydrogen at 1200°C are shown in Figures 2 and 3 correspondingly. Mn_2O_3 and Mn_3O_4 oxides, which were the main manganese-containing phases in the ore, became undetectable by XRD after 15 min sintering in helium, and quartz peak height decreased significantly. Tephroite became a dominant phase with traces of quartz. XRD spectra of the GE-PS

ore sintered further for 30 min revealed partial decomposition of tephroite (Mn_2SiO_4) to MnO and rhodonite ($MnSiO_3$). Both, tephroite and rhodonite contained iron oxide.

Different behaviour of the ore was observed in the process of sintering at 1200°C in hydrogen. 10 min sintering resulted in the reduction of manganese oxides to MnO and iron oxides to metallic iron, and formation of tephroite. After 20 min sintering, major phases identified by XRD were quartz, MnO and tephroite. Further formation of tephroite proceeded by reaction of MnO with silica. This process was slow; XRD spectra of a sample sintered for 60 min revealed the same phases as in the sample sintered for 20 min, although the height of MnO peaks decreased and height of tephroite peaks increased with increasing sintering time. Rhodonite was not detected in the sintered sample, while quartz peaks in the XRD spectra remained strong even after 1 hour of sintering (Figure 3); quartz was also visible in optical images.

Reduction of higher manganese oxides to MnO and iron oxides to Fe corresponds to 40% of total reduction of manganese and iron oxides in the ore (calculated from the weight loss). The degree of reduction of GE-PS ore in hydrogen at 1200°C was about the same as at 1000°C. In sintering in an inert atmosphere, reduction of MnO_2 at 1000°C did not go beyond Mn_3O_4.

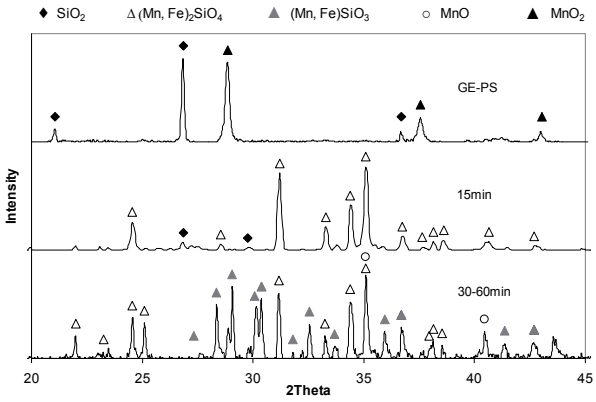

Figure 2: XRD patterns of preheated in air GE-PS samples further sintered in helium at 1200°C.

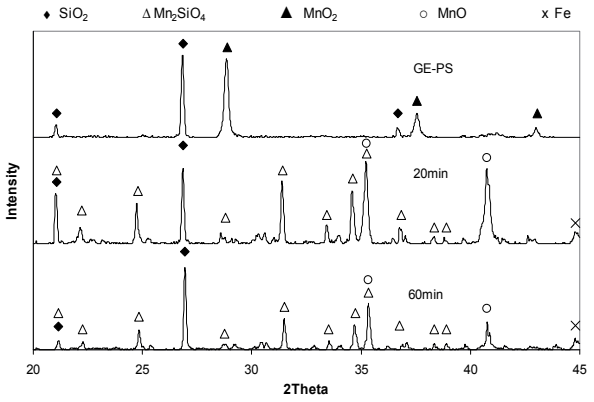

Figure 3: XRD patterns of preheated in air GE-PS samples further sintered in hydrogen at 1200°C.

3.2 Ore Reduction

Reduction curves for the GE-PS ore obtained in non-isothermal experiments in helium and hydrogen are presented in Figures 4 and 5 correspondingly. The first reduction stage in helium which was conversion of MnO_2 and Mn_2O_3 to Mn_3O_4 and higher iron oxides to "FeO" started at about 400°C. In the second reduction stage, Mn_3O_4 was reduced to MnO and iron oxides to metallic iron. These two stages were indistinguishable and combined into one in reduction in hydrogen, which began at 300°C.

Higher manganese and iron oxides were reduced in a helium atmosphere by carbon with formation of CO_2 at temperatures below about 1000°C; at higher temperatures, CO was formed. The CO_2 evolution curve had a major peak at 920°C, which was closely followed by the CO peak at about 950°C. These peaks are of the same origin and are distinguished only as a result of changing conditions for the Boudouard reaction.

Conversion of manganese oxides to MnO and iron oxides to metallic iron at temperatures above about 1000°C overlapped with reduction of MnO to ferro-manganese carbide. This process slowed down at about 1180°C, when molten slag started to form. The rate of MnO reduction from molten slag peaked up at 1400°C. The final extent of reduction was above 100% indicating reduction of silica from the molten slag at high temperatures.

In reduction experiments in hydrogen (Figure 5), higher manganese oxides were reduced to MnO and iron oxides to Fe by hydrogen at temperatures below 900°C with the formation of water vapour; at

higher temperatures, reduction was predominantly proceeded by carbon. The rate of this stage in hydrogen was faster than in helium; it was completed at around 1150°C before the slag started to form.

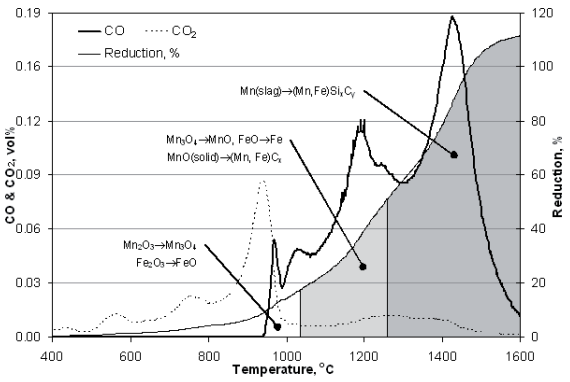

Figure 4: Non-Isothermal reduction of GE-PS ore in helium. Ramp rate 5°C/min.

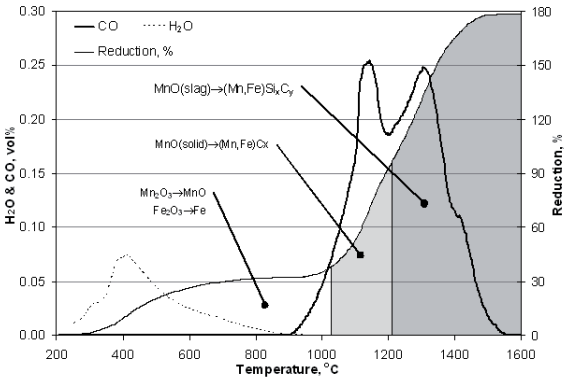

Figure 5: Non-Isothermal reduction of GE-PS ore in hydrogen. Ramp rate 5°C/min.

Isothermal reduction of GE-PS was studied at 1100-1200°C. Reduction curves obtained at these temperatures in argon, helium and hydrogen are presented in Figure 6. For comparison, reduction curves for pure MnO in hydrogen are also shown in the figure.

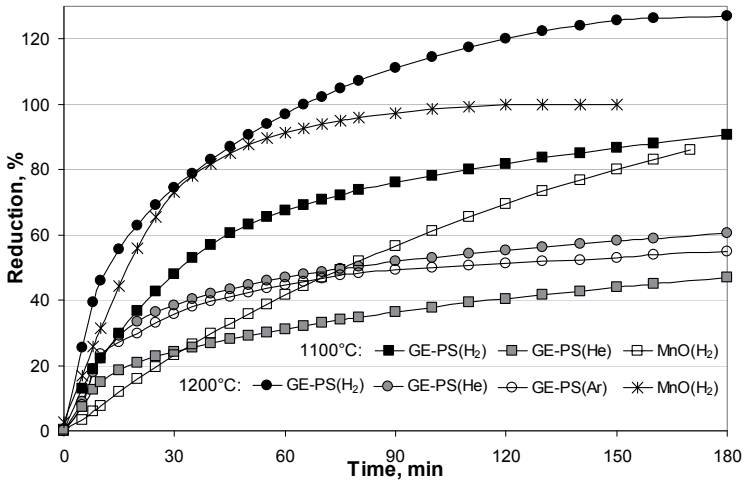

Figure 6: Reduction of GE-PS ore in hydrogen, helium and argon atmospheres and reduction of MnO oxide in hydrogen at 1100 and 1200°C.

The rate and degree of reduction of GE-PS ore increased with increasing temperature. Reduction was faster in helium than in argon at 1100°C; the difference between reduction in Ar and He at 1200°C was insignificant. At both temperatures, reduction of GE-PS ore was much faster in hydrogen than in helium. In the process of carbothermal reduction of GE-PS ore in hydrogen at 1200°C, silica was reduced. Reduction of GE-PS ore in hydrogen was faster than of MnO, particularly at 1100°C.

The main stages of carbothermal reduction of GE-PS ore in hydrogen at 1100°C can be identified from XRD analysis shown in Table 3. Reduction of the ore started with fast reduction of high manganese oxides to MnO and reduction of iron oxides to metallic iron; most of the SiO_2 phase remained intact. Tephroite and traces of ferromanganese carbide were detected after 10 min of reduction. Manganese oxides were reduced to ferromanganese carbide $(Mn, Fe)_7C_3$ and reacted with silica to form tephroite; MnO was not detected in XRD spectra after 60 min. Further reduction included reduction of manganese oxide from tephroite.

Table 3 Phases detected by XRD at different stage of reduction of GE-PS ore in hydrogen at 1100°C and 1200°C.

1100°C		1200°C	
Time, min	Phase detected	Time, min	Phases detected
0	Mn_2O_3, Mn_3O_4, SiO_2	0	Mn_2O_3, Mn_3O_4, SiO_2
10	MnO, SiO_2, Mn_2SiO_4, $(Mn, Fe)_7C_3$	15	SiO_2, Mn_2SiO_4, $(Mn, Fe)_7C_3$
30	MnO, SiO_2, Mn_2SiO_4, $(Mn, Fe)_7C_3$	30	SiO_2, $(Mn, Fe)SiO_3$, $(Mn, Fe)_7C_3$
60-180	SiO_2, Mn_2SiO_4, $(Mn, Fe)_7C_3$	60	SiO_2, $(Mn, Fe)SiO_3$, $(Mn,Fe)_5SiC$
		150	SiO_2, $(Mn,Fe)_{22.6}Si_{5.4}C_4$, $(Mn,Fe)_5Si_3$

Carbothermal reduction of the GE-PS ore at 1200°C was affected by formation of molten slag. Ferromanganese carbide $(Mn, Fe)_7C_3$ was detected after first 10-15 min of reaction. MnO was not observed on the XRD spectrum of a sample after 15 min of reaction. Major phases at this stage were tephroite and silica. SEM and EDS analyses identified two types of particles formed at this stage. The first type contained ferromanganese carbide enriched with iron, tephroite and $MnO\text{-}SiO_2\text{-}Al_2O_3$ slag. The second type of particles in addition to these phases contained MnO, which was virtually encapsulated into the bulk of the slag phase. These particles contained higher MnO and lower iron content in comparison with particles of the first type[12]. High iron content in the ore particles stimulated nucleation and growth of the metal phase. Further reduction of MnO proceeded from the slag. Tephroite was converted to rhodonite by the reaction:

$$2MnO{\cdot}SiO_2 \rightarrow MnO{\cdot}SiO_2 + MnO \quad (1)$$

MnO formed by this reaction was reduced to the carbide phase.

Silicon was also observed in the metallic phase from the beginning of reduction[12]. Carbides $(Mn, Fe)Si_xC_y$ of different compositions were identified by EMPA after 30 min of reduction. After 30-40 min from the beginning of reduction, carbon in the manganese-iron carbide $(Mn, Fe)_7C_3$ was gradually replaced by silicon reduced from the slag phase. This process was very slow; when reduction lasted longer than 150 min, ferro-manganese silicide $(Mn, Fe)_5Si_3$ was formed. The relationship between carbon and silicon concentrations followed a trend established for manganese alloys[13].

4 DISCUSSION

4.1 Sintering of GE-PS ore

Equilibrium phases in Groote Eylandt GE-PS ore sintered in the temperature range 800-1200°C in air and hydrogen, en are presented in Table 4.

Major equilibrium phases in GE-PS ore in air at 800°C are bixbyite with 87.4 wt% Mn_2O_3 and quartz. Potassium at this temperature is in the composition of leucite, which has a high melting temperature. When temperature is increased to 1000°C, Mn_2O_3 of bixbyite and silica form rhodonite which is a major equilibrium phase together with bixbyite, in which Mn_2O_3 concentration decreased to 79.4 wt%. Silica, alumina and potassium oxide form liquid slag with high SiO_2 and K_2O concentration. The slag becomes a major phase at 1200°C; bixbyite is converted to tetragonal spinel, predominantly $(Mn,Fe)_3O_4$, which is the second major phase in GE-PS ore at this temperature in air.

Major equilibrium phases in the GE-PS ore in reducing atmosphere at 800°C and 1000°C are rhodonite and tephroite which form liquid slag at 1200°C.

Table 4 Equilibrium phases in Groote-Eylandt siliceous fines heated in air and H_2 to 800-1200°C

Atmosphere	Temperature, °C	Phases
Air	800	**Bixbyite** $(Mn, Fe)_2O_3$**, 87.4% Mn_2O_3**, **Quartz**, garnet $Mn_3Al_2Si_3O_{12}$, leucite $KAlSi_2O_6$, $BaO.SiO_2$ (wollastonite $(Ca,Mn)SiO_3$, 11.8% $MnSiO_3$)
	1000	**Rhodonite $MnSiO_3$, Bixbyite, 79.4% Mn_2O_3, garnet** $Mn_3Al_2Si_3O_{18}$, Liquid slag (79.8% SiO_2, 13.8% K_2O, 6.43% Al_2O_3), $BaO.SiO_2$.
	1200	**Liquid slag** (51.6% MnO, 42.5% SiO_2, 4.25% Al_2O_3, 0.66% K_2O), **Tetragonal spinel $(Mn,Fe)_3O_4$,** Rhodonite, 98.5% $MnSiO_3$, $BaO.SiO_2$.
H_2	800	**Rhodonite, 98.7% $MnSiO_3$**, **tephroite Mn_2SiO_4**, garnet $Mn_3Al_2Si_3O_{12}$, Fe, leucite $KAlSi_2O_6$, $BaO.SiO_2$.
	1000	**Rhodonite, 99.1% $MnSiO_3$, tephroite Mn_2SiO_4**, garnet $Mn_3Al_2Si_3O_{12}$, Fe, leucite $KAlSi_2O_6$, $BaO.SiO_2$.
	1200	**Liquid slag** (56.8% MnO, 38.6% SiO_2, 3.70% Al_2O_3, 0.50% K_2O), Fe, $BaO.SiO_2$.

Note: In bold: major phases; in brackets: minor phases, less than 1 wt%; phases are presented in the descending (mass) order.

XRD analysis of a sample sintered in air at 1000°C detected quartz, which was also observed in a sample sintered in hydrogen at 1000-1200°C. Apart from quartz, the XRD analysis of GE-PS ore sintered in air identified Mn_3O_4 and Mn_2O_3 phases. Obviously, equilibrium was not reached during 3 hours exposure at 1000°C in air. It was not reached in the process of sintering at 1200°C either. XRD analysis of a sample sintered in hydrogen showed tephroite and MnO phases which were probably formed in the process of slag solidification. However, a different situation was observed when GE-PS ore was sintered at 1200°C in helium (Figure 2). In a sample exposed to helium for 15 min, a major phase in the XRD spectra was tephroite; in samples sintered for 30-60 min, rhodonite, tephroite and MnO phases were identified. Quartz was not observed in the XRD spectra. It can be suggested that upon heating of GE-PS ore in an inert atmosphere at 1200°C, quartz was dissolved into the liquid slag. Rhodonite, tephroite and MnO phases observed in the XRD spectrum, were, probably, formed upon solidification of liquid slag. When the ore was heated in hydrogen, reduction of higher manganese oxides to the MnO phase and formation of tephroite retarded formation of liquid slag.

4.2 Reduction of GE-PS ore

The effect of temperature on the rate of carbothermal reduction of manganese ore agrees with literature data; the reduction rate increases with increasing temperature. Data of thermo-gravimetric analysis of reduction of Groote Eylandt siliceous manganese ore in argon by Ostrovski and Webb[14] at 1200°C are in good agreement with this work.

Carbothermal reduction of MnO in argon, helium and hydrogen was considered in [10]. Carbothermal reduction of metal oxides proceeds via the gas phase. The carbothermal reduction of MnO to carbide Mn_7C_3 in an inert gas is presented as:

$$7MnO + 13CO = Mn_7C_3 + 10CO_2 \quad (2)$$

CO_2 is converted back into CO by the Boudouard reaction.

The rate of the overall MnO reduction is suggested to be limited by the interfacial Boudouard reaction [15, 16], or by mass transfer of CO_2 within the porous bed of the solid reactant mixture to the carbon particles[17].

The MnO carbothermal reduction was fastest in hydrogen, and was faster in helium than in argon. The strong effect of gas atmosphere on the rate of manganese oxides reduction indicates that external and internal mass transfer of gaseous species involved in the reaction play an important role in the reduction kinetics. The difference between Ar and He is the degree of resistance that they impose onto the diffusivity of other gaseous species. Diffusivity of CO in helium and argon, calculated

using the Chapman-Enskog formula [18] at 1400°C and 1 atmosphere is 16.9 cm^2sec^{-1} and 3.6 cm^2sec^{-1} respectively. The difference is a factor of 4.7.

Diffusivity of CO in hydrogen and helium is about the same, therefore internal and external mass transfer is not a factor distinguishing carbothermal reduction of manganese oxides in hydrogen and helium. However, hydrogen is involved in the reduction process. Hydrogen reduces higher manganese oxides to MnO and iron oxides to metallic iron in the first reduction stage. Reacting with carbon it forms methane (Reaction 3) which can reduce MnO to Mn_7C_3 by Reaction (4):

$$C + 2H_2 = CH_4 \quad (3)$$

$$7MnO + 10CH_4 = Mn_7C_3 + 20H_2 + 7CO \quad (4)$$

Although partial pressure of methane in the gas phase is low (0.01-0.03 atm in the range of experimental temperatures), the carbon activity of the gas phase in equilibrium with graphite is 1, which is sufficient for manganese carbide formation. In general, solid-gas reactions are faster than solid-solid reactions. Methane may act as a means for carbon transportation, which accelerates the overall reduction process.

At temperatures below 1300°C, partial pressure of methane is significantly higher than partial pressure of CO_2 (about 2 orders in magnitude at 1200°C). Therefore following analysis in ref.[17], methane mass transfer from carbon to MnO is expected to be much faster than CO_2 mass transfer from MnO to graphite. The chemical reaction with intermediate methane is also expected to be faster than with CO_2 as it depends on the partial pressure of a reactant.

Formation of a liquid phase in the process of reduction of Groote Eylandt ore was a significant factor affecting the ore reduction. In reduction of GE ore by methane containing gas studied by Anacleto et al. [19], the extent and rate of reduction significantly decreased with increasing temperature from 1100°C to 1200°C; the degree of reduction of this ore at 1200°C was slightly above 50% after 5 hours of reaction. This was attributed to the formation of a liquid phase and decrease in the interfacial reaction area with blockage of methane-hydrogen gas access to the ore interior. Doping of the ore with lime (10-15% CaO) increased the ore melting temperature and significantly enhanced reduction rate and extent at 1200°C [19].

Carbothermal reduction behaviour of ores was different from that observed in reduction by methane-containing gas. The major difference between these processes is obvious: carbon is intimately mixed with oxides in the carbothermal reduction, while in reduction by CH_4-H_2 gas, carbon is delivered to the ore interior from the gas phase. This process includes methane adsorption, which depends strongly on the available surface sites.

Equilibrium phases in the carbothermal reduction of GE-PS ore in H_2 calculated using FactSage software are presented in Table 5. The ore was mixed with excess graphite; equilibrium phases were calculated at 1100°C and 1200°C, at the same temperatures at which their reduction was studied experimentally.

Equilibrium phases formed at 1100°C included rhodonite (a major phase), carbide $(Mn,Fe)_7C_3$, molten slag, leucite and $BaO.SiO_2$. In accordance with equilibrium calculations (Table 5), tephroite was converted to rhodonite and manganese carbide ($2MnO{\cdot}SiO_2$ → $MnO{\cdot}SiO_2$ +MnO→ $MnO{\cdot}SiO_2$ +Mn_7C_3). Amounts of leucite and barium silicate in the equilibrium phases were below the detectable level by XRD. Major phases detected by XRD analysis (Table 3) included tephroite and carbide $(Mn,Fe)_7C_3$. Obviously, equilibrium was not reached in the reduction at 1100°C, and MnO of tephroite was not reduced. The slag phase upon crystallisation formed a poorly crystallised phase which was unidentified by XRD.

Table 5 Equilibrium phases in GE-PS ore – graphite mixture heated in H_2 atmosphere to 1100-1200°C

Temperature, °C	Phases
1100	**$MnSiO_3$**; Slag (47.6% MnO, 43.8% Al_2O_3, 43.8% SiO_2) $(Mn,Fe)_7C_3$ (65.8% Mn, 25.7% Fe, 8.53% C); Leucite $KAlSi_2O_6$; $BaO.SiO_2$.
1200	**Liquid metal (73% Mn, 14.3% Fe, 10.6% Si, 2.04% C)**; Garnet $Mn_3Al_2Si_3O_{12}$; Mn_7C_3; Slag (0.31% MnO, 6.37% Al_2O_3, 82.5% SiO_2, 10.1% K_2O); $BaO.SiO_2$; $(Mn,Ca)SiO_3$.

Note: In bold: major phases. Both samples contained graphite.

Liquid metal was the major equilibrium phase at 1200°C; it crystallised to carbides and silicide, which were observed experimentally. The calculated amount of molten slag in equilibrium phases was less than 10 wt%. It contained only 0.31 wt% MnO; the main slag's component was silica. Manganese oxide was mainly present in the form of garnet $Mn_3Al_2Si_3O_{12}$. MnO reduction at equilibrium reached a high degree, above 90%. No manganese oxide was detected in the reduced samples by XRD analysis. The metal at equilibrium contained high silicon concentration, 10.6 wt% (calculated). High silicon content in the alloy produced by carbothermal reduction of GE-PS ore in hydrogen at 1200°C was observed experimentally. It should be mentioned that in high carbon ferromanganese which is produced at about 1500°C, silicon content is below 1 wt%; typical silicomanganese, which production requires 1650°C, contains 16-19% Si. This confirms that Groote Eylandt manganese siliceous fines is an appropriate ore for production of silicomanganese.

5 CONCLUSIONS

Groote Eylandt manganese siliceous ore is characterised by very high silica, 34.4 wt%. Major phases identified by XRD and EPMA analyses were pyrolusite, iron silicate, cryptomeline and quartz. Upon sintering at 1000°C, MnO_2 was reduced to Mn_2O_3 and Mn_3O_4 in air and to Mn_3O_4 in argon. Sintering of manganese ores in hydrogen at 1000°C reduced higher manganese oxides to MnO and iron oxides to metallic iron.

In the process of sintering of the GE-PS ore at 1200°C in helium, tephroite was formed by reaction of Mn_2O_3 and Mn_3O_4 oxides with silica; tephroite was partially decomposed to MnO and rhodonite by extending sintering time to 30 min. When this ore was sintered in hydrogen, higher manganese oxides were quickly reduced to MnO with formation of tephroite. Further formation of tephroite was by reaction of MnO with quartz; rhodonite was not observed in the sample sintered for 1 hour.

Manganese oxide was predominantly reduced from tephroite and rhodonite; quartz was still detected after 150 min of reduction. The final slag contained alumina, silica and manganese oxides.

Carbothermal reduction of manganese ore proceeded in two main stages. In the first stage high manganese oxides were reduced to MnO and iron oxides to metallic iron. The second stage involved reduction of manganese oxides to ferromanganese carbide. The effects of temperature and gas atmosphere on the reduction of GE-PS can be summarised as follows:

The rate and degree of reduction increased with increasing temperature from 1100°C to 1200°C. Reduction was faster in helium than in argon at 1100°C; the difference was insignificant in reduction at 1200°C. Reduction was much faster in hydrogen than in helium;

In the process of carbothermal reduction of ores in hydrogen at 1200°C, silica was reduced.

Faster reduction of manganese ore in hydrogen than in inert gases was explained by formation of methane which was involved in the reduction process.

The degree of manganese oxide and particularly silica reduction was very high at the reduction temperature of 1200°C. Silica was reduced to the carbide phase; ferromanganese silicides were also formed. The metallic phase in the reduced sample after 180 min of reduction contained 1.2-1.9 wt% C and 21-22 wt% Si.
FactSage calculations correctly predicted major phases formed in the process of heating and reduction of GE-PS ore.

6 ACKNOWLEDGEMENTS

This research was supported under Australian Research Council Linkage Project funding scheme (project number LP0560703).

7 REFERENCES

[1] Olsen S., Tangstad M., Lindstad T. “Production of Manganese Ferroalloys”, Tapir Academic Press, Trondheim, Norway, 2007.
[2] Yastreboff M., Ostrovski O. and Ganguly S. “Effect of Gas Composition on the Carbothermic Reduction of Manganese Oxide”, ISIJ Int., 43 (2003), 161-165.
[3] Yastreboff M. M. ‘‘Mechanism of Carbothermic Reduction of Manganese Oxide from Manganese Ore and Ferromanganese Slag”, PhD thesis, University of New South Wales, Sydney, Australia, 2001.
[4] Grimsley W.D., See J.B. and King R.P. “The Mechanism and Rate of Reduction of Mamatwan Manganese Ore Fines by Carbon”, J. S. Afr. Inst. Min. Metall., 10 (1977), 51-62.
[5] Yastreboff M., Ostrovski O. and Ganguly S. ‘‘Carbothermic Reduction of Manganese from Manganese Ore and Ferromanganese Slag”, Proc. 8th Int. Ferroalloys Congress, Beijing, China, 1998, June 7-10, 263-270.
[6] Ostrovski O., Olsen S. E., Tangstad M. and Yastreboff M. “Kinetic Modelling of MnO Reduction from Manganese Ore”, Can. Metall. Q., 41 (2002), 309-318.
[7] Gasik M. I. “Manganese”, Metallurgiya, Moscow, 1992 (in Russian).
[8] Kononov R., Ostrovski O. and Ganguly S. “Carbothermal Solid State Reduction of Manganese Ores: 1. Manganese Ore Characterisation”, ISIJ Int., 49 (2009), 1099-1106.
[9] Akdogan G. and Eric R. H. “Carbothermic Reduction Behaviour of Wessel Manganese Ores”’ Miner. Eng., 7 (1994), 633–645.
[10] Kononov R., Ostrovski O. and Ganguly S. “Carbothermal Reduction of Manganese Oxide in Different Gas Atmosphere”, Metall. Mater. Trans. B, 39B (2008), 662-668.
[11] Tang, K., Olsen, S.E., “Computer Simulation of Equilibrium Relations in Manganese Ferroalloy Production”, Metallurgical and Materials Transactions B, 37B (2006), 599-606.
[12] Kononov R., Ostrovski O. and Ganguly S. “Carbothermal Solid State Reduction of Manganese Ores: 3. Phase Development”, ISIJ Int., 49 (2009), 1115–1122.
[13] Anacleto N., Ostrovski O. and Ganguly S. “Carbon Solubility and Phase Composition of Silicomanganese”, Steel Res. Int., 77 (2006), 227-233.
[14] Ostrovski O. and Webb T. “Reduction of Siliceous Manganese Ore by Graphite”, ISIJ Int., 35 (1995), 1331-1339.
[15] Rankin W. J. and Van Deventer J. S. J. “The Kinetics of the Reduction of Manganous Oxide by Graphite”, J. S. Afr. Inst. Min. Metall., 80 (1980), 239-247.
[16] Tereyama K. and Ikeda M. “Study on Reduction of MnO with Carbon by Effluent Gas Analysis Method”, Trans. Jpn. Inst. Met., 26 (1985), 108–114.
[17] Rankin W. J. and Wynnyckyj J. R. “Kinetics of Reduction of MnO in Powder Mixtures with Carbon”, Metall. Materials Trans. B, 28B (1997), 307-319.
[18] Bird R., Stewart W. and Lightfoot E. “Transport Phenomena”, John Wiley and Sons, New York, 1960.
[19] Anacleto N., Ostrovski O. and Ganguly S. “Reduction of Manganese Ores by Methane-containing Gas”, ISIJ Int., 44 (2004), 1615–1622.